Comparing planktonic-to-benthic (P/B) ratio signals to modern sea ice proxies at the Yermak Plateau, Arctic Ocean, during the last 160 ka

Anton Almgren

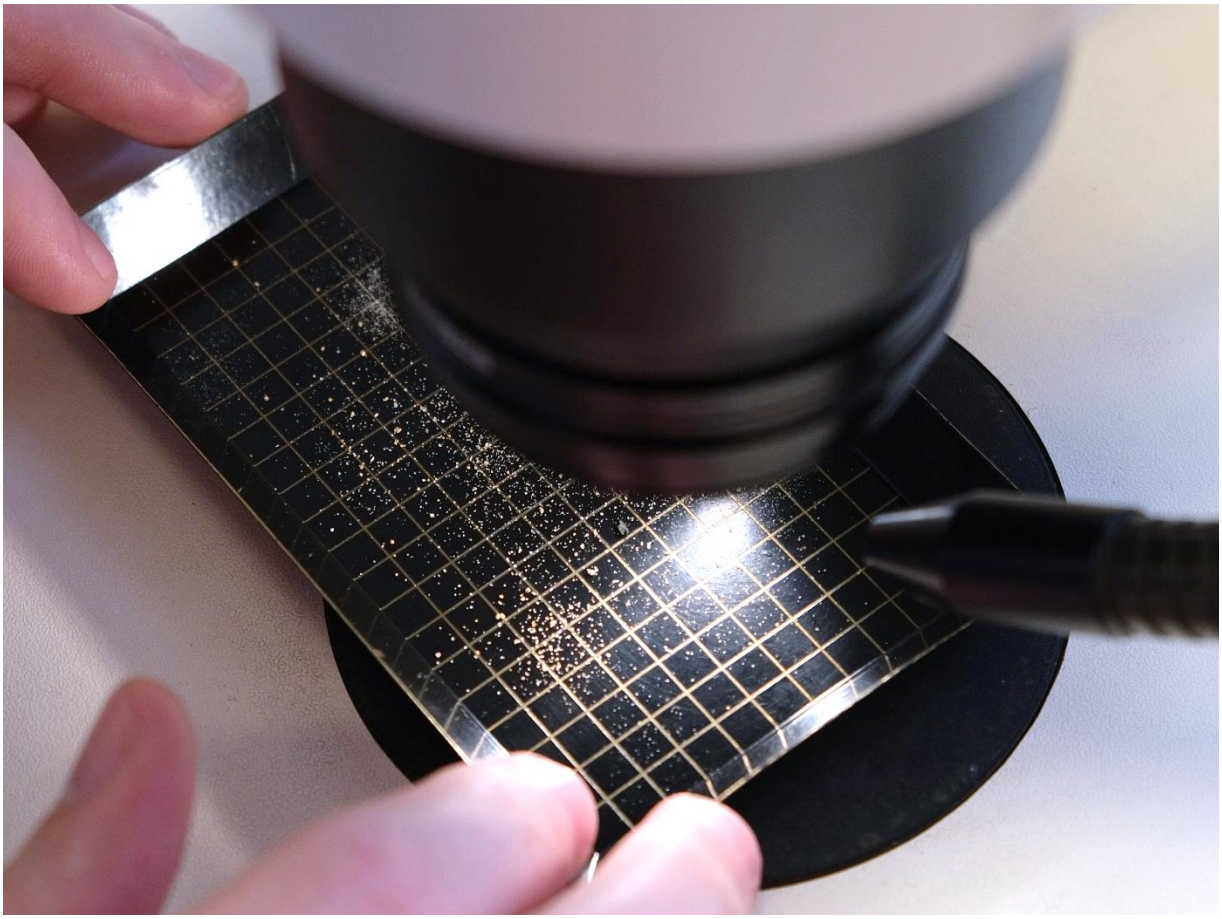

Department of Physical Geography
Department of Geological Sciences
Degree 15 HE credits
Geovetenskap
Earth Science (180 credits)
Spring term 2020
Supervisors: Hellen Coxall & Matthew O'Regan
Examiners: Flor Vermassen & Alasdair Skelton

Stockholms universitet

Comparing planktonic-to-benthic (P/B) ratio signals to modern sea ice proxies at the Yermak Plateau, Arctic Ocean, during the last 160 ka

Anton Almgren

Abstract

The Arctic Ocean is presently experiencing rapid changes in terms of sea ice extent. Palaeoceanographic records of past ocean conditions and sea ice variability provides an important context to understanding present and future developments in the Arctic Ocean. Global paleorecords based on stable isotope analysis of foraminifera have already given us, in some cases, millions of years of paleoceanic and paleoclimatic data, and modern sea ice proxies are still being developed. In this study relative foraminiferal abundance counts are performed on dry sediment samples from a Polarstern core PS92/045-2 at the Yermak Plateau, and a P/B ratio (planktonic-to-benthic ratio) is generated, which is then compared to the signals of a modern biomarker based sea ice proxy (IP_{25}), in a reconstruction previously done on nearby Polarstern core PS92/039-2 (Kremer et al. 2018). The P/B ratio, which is a relatively easily obtainable metric, has previously been used to make inferences on sea ice conditions, with low P/B ratios (below 1:1) interpreted as indicating less sea ice extent, and higher values indicating more extensive sea ice cover. This study concludes that there are some general common patterns between P/B ratio, absolute foraminiferal abundances and IP_{25} signals, but that the use of P/B ratio as a sea ice proxy probably cannot reliably be embraced with this specific core and location at the Yermak Plateau.

Keywords

Seafloor sediments
Foraminifera
Abundance counts
P/B ratio
Proxy comparison
Sea ice variability
Yermak Plateau
Arctic Ocean

Contents

1. Introduction

Arctic sea ice, climate and foraminifera

Arctic sea ice is a critical part of the Earth's climate system. Presently, some variables that may be influenced by Arctic sea ice include the global sea level (Jakobsson et al. 2016; Osborne et al. 2017), the global energy balance by alteration of Earth's surface albedo (Kashiwase et al. 2017), the ocean-atmosphere heat and moisture exchange by insulation of the ocean surface (Zheng et al. 2019), the conditions of arctic ecosystems and primary production by facilitating or limiting habitats (Arrigo and van Dijken 2015; Cusset et al. 2019) and the thermohaline circulation (Rashid et al 2011). Some major variables that in turn presently affect sea ice variability include orbital scale climactic forcing (Marzen et al. 2016), the polar amplification feedback of a reduced surface albedo (Kashiwase et al. 2017) and inflow of warmer Pacific and Atlantic Water (Ruediger Stein et al. 2017; Spielhagen et al. 2011).

Although the interplay of these and many more external and internal variables make arctic sea ice variability a complex matter, there is an observable trend through the past four decades that shows a shrinking sea ice cover ('National Snow and Ice Data Center |' n.d.). Because of the weight of the role that arctic sea ice plays in Earth's climate stability, this trend is being followed closely as some researchers predict a seasonally ice-free arctic ocean as soon as mid-century, which is considered to be an unmatched development over the last few thousand years (Polyak et al. 2010; Notz and Stroeve 2018). Although observational data on sea ice in the Arctic only exists for the past few decades, several proxy and multi-proxy records of past oceanographic conditions, climate and other useful information have been constructed to, in some cases, cover the last several million years (Lisiecki and Raymo 2005). Palaeoceanographic records provide an important historical context to better understand the present and future developments in the Arctic.

A powerful source of this kind of information exists in microfossils of foraminifera derived from marine sediment cores. Foraminifera are single-celled, shell-building eukaryotes that are present in both the water column as planktonic foraminifers, and in the benthic zone as benthic foraminifers. Foraminifers can build tests (shells) of different material available to them such as rock and mineral grains (agglutinated tests), or by secretion of calcium carbonate. A common feature of foraminifer tests are chambers, chambers are added as the foraminifer grows. When foraminifers die, their tests remain and accumulate on the seafloor over time (Wetmore 1996).

Oxygen stable isotope analysis of the calcareous tests of foraminifers, as well as studies of the presence, relative abundances and assemblages of different foraminifera species in marine sediment cores can be used to make inferences on plaeoceanic conditions such as water temperature, salinity and the presence of sea ice (Wetmore 1996; Cronin et al. 2008; Lagoe 1977). For example, in a massive effort, Lisiecki and Raymo (2005) created a global paleorecord based on benthic foraminiferal $\delta^{18}O$ as a water temperature and global sea ice volume proxy thereby identifying 24 marine isotope stages (MIS). Marine isotope stages represent glacial (even numbered) and interglacial stages (odd numbered) in geologic time, and provides the principal globally correlative chemo-chronostratigraphic method for dating paleorecords (Lisiecki and Raymo 2005).

In this project, foraminiferal abundance data is generated from a sediment core drilled on the Yermak Plateau, Arctic Ocean, and this data is subsequently compared to data from a more technical biomarker-based sea ice reconstruction on a nearby sediment core by Kremer et al. (2018). The goal is to compare the two methods, and specifically to see whether the ratio between planktonic and benthic foraminiferal abundances can be used to infer what kind of sea ice conditions the Yermak Plateau has experienced during the last 160 ka.

2. Background

2.1 Regional setting

The Yermak Plateau protrudes from the northwest corner of the Svalbard continental margin. It covers a latitudinal range of about 80’00° - 83’00° N and is nearly centered on the prime meridian (Geissler et al. 2011). It is located in the Eurasian Basin directly north of the Fram Strait which interfaces the Arctic Ocean and the Greenland and Norwegian seas to the south. The Fram Strait is also the only deep water connection between the Arctic Ocean and the rest of the world’s oceans (Klenke and Schenke 2002). The bathymetry of the Yermak Plateau influences the West Spitsbergen Current (WSC) that brings warmer saline Atlantic Water (AW) into the Arctic Ocean. As the WSC enters the Arctic Ocean, it splits into three different branches, one that goes westward into the Return Atlantic Current, and two branches that are divided by the Yermak Plateau and flows on either side of it into the Arctic Ocean (Nilsen et al. 2016). West of the WSC the East Greenland Current exports cold and low-salinity Arctic Ocean water masses as well as Arctic sea ice out into the Greenland Sea and the North Atlantic (Martin and Wadhams 1999). The Svalbard Barents Sea Ice Sheet (SBIS) has historically, during glaciations, extended toward the Svalbard continental shelf (Ingólfsson and Landvik 2013). An illustration of the regional geography, bathymetry can be seen in Figure 1 below. The two sediment cores investigated in this study are

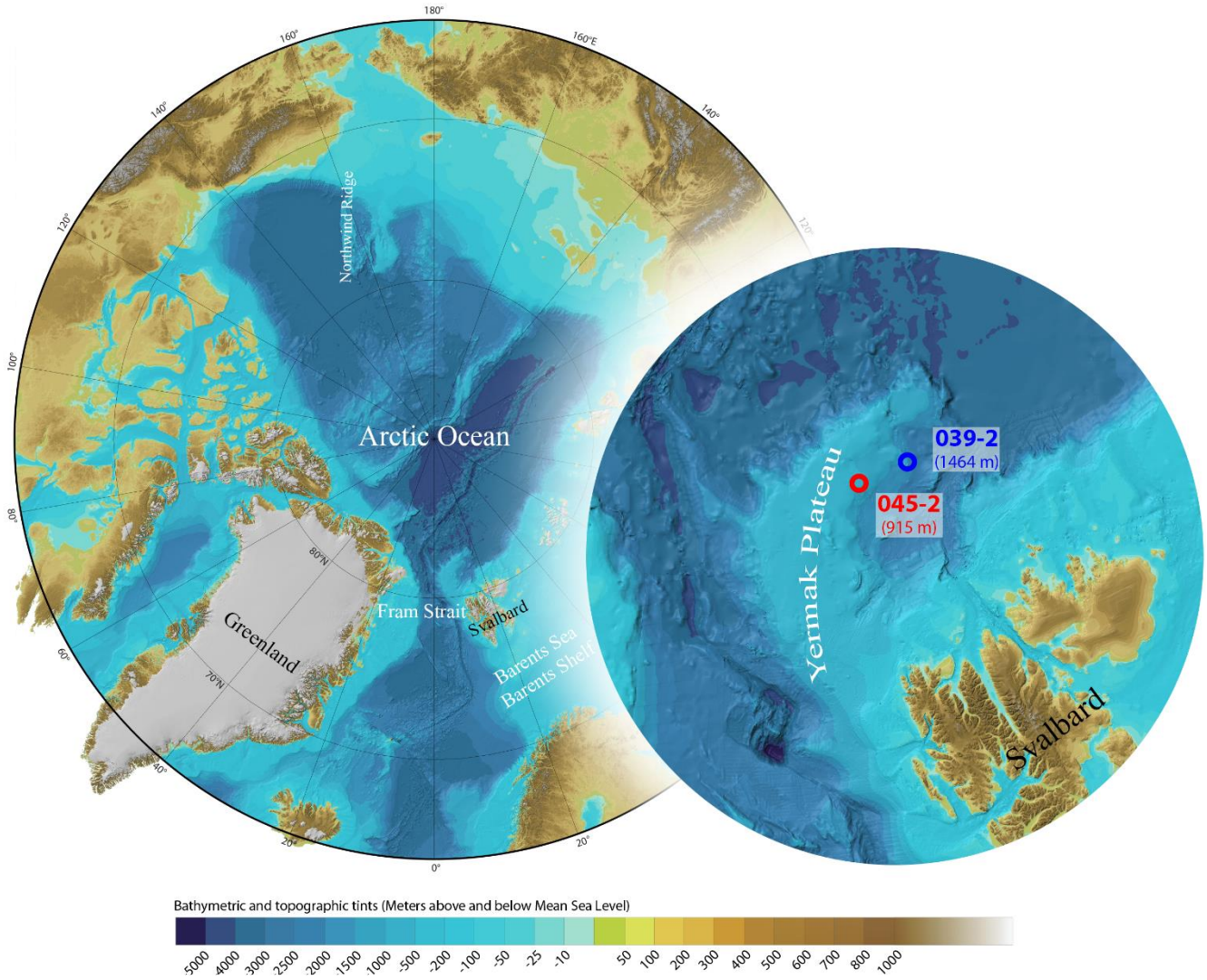

***Figure 1**: The regional setting of the Yermak Plateau, including bathymetry and the core sites with water depth (m). Note: The core sites are not georeferenced to the basemap, locations are approximate. Basemap: IBCAO (Jakobsson et al. 2012).*

PS92/045-2 and PS92/039-2 (henceforth referred to as 045-2 and 039-2 respectively) cored during the 2015 expedition PS92 of R/V Polarstern (Peeken 2016). Some additional information about these cores can be found in Table 1 below.

Table 1. *Information on the sediment cores referenced in this study (Peeken 2016).*

Core	Core method	Lat	Long	Water depth (m)
PS92/045-2	Gravity core	81° 53 60' N	9° 46 13' E	915
PS92/039-2	Kasten core	81° 56 99' N	13° 49 70'E	1464

2.2 Foraminifera in the Arctic Ocean

Compared to lower latitude and equatorial waters the foraminiferal diversity in the polar regions is very low. A single species, *Neogloboquadrina pachyderma* sin., dominates most of the planktonic communities in the Arctic Ocean. In surface sediments at the eastern end of the Fram Strait the planktonic assemblage can include small percentages of the sub-polar species *Turborotalita quinqueloba* and the dextral coiling *N. pachyderma* dex. This is thought to be because of the proximity to warmer Atlantic Water (WSC) and seasonally ice-free conditions. *T. quinqueloba* are rare or absent in surface sediments in the >125 µm fraction due to their thin tests being more vulnerable to carbonate dissolution. Although presence of *N. pachyderma* typically decreases during glacial stages, especially in the western Arctic, it can in the Eurasian Basin show increased abundances in glacial intervals, which again is attributed to presence of warmer Atlantic Water, but also to the formation of polynyas which can create large areas of open ocean conditions (Stein 2008).

The benthic component of arctic foraminifera is much more diverse than the planktonic. A couple of recognized influences on the distribution of benthic foraminifera in the Arctic Ocean include surface-water productivity and sea ice conditions (Stein 2008). Lagoe (1977) and Husum (2015) are two notable contributions to the study of modern benthic foraminifers in the Arctic (Lagoe 1977; Husum et al. 2015). Two different types of benthic foraminifera are considered in this study, agglutinated and calcareous benthic foraminifera. The key difference between these two categories is that the former build their tests by secreting calcium carbonate, while the latter build their tests by cementing mineral grains or other particles together (Wetmore 1996) While keeping fossil preservation dynamics in mind, including carbonate dissolution, it has been suggested that agglutinated benthic foraminifera dominate during seasonally ice-free conditions (Cronin et al. 2008).

While ostracodes are not members of the Foraminifera subphylum, but forms their own class in the Crustacean subphylum, they can also form calcareous shells that tend to be fossilized and therefore also serves as a potential paleorecord based on their species distribution and assemblages (Cronin et al. 2008).

Because of the diversity and equally diverse ecological preferences of foraminiferal species, their distribution, assemblages, presence and abundances in marine sediment cores can be used to infer past oceanic conditions (Lagoe 1977; Polyak et al. 2013; Husum et al. 2015; Chauhan et al. 2014). The relationship between planktonic and benthic foraminiferal abundances (P/B-ratio) has previously been subject to study in the Arctic Ocean, where its usefulness in determining water depth (proximity to continental shelf), food supply, carbonate dissolution and surface productivity have been considered (Berger and Diester-Haass 1988; Scott and Vilks 1991; Schell et al. 2008; Polyak et al. 2013). Polyak et al. (2013) in a study on sediment cores from the Northwind Ridge (Figure 1) associates a low P/B ratio (meaning *more benthic* than planktonic foraminifers) to seasonally ice free conditions and a high P/B ratio (meaning *more planktonic* than benthicc foraminifera) to perennial sea ice cover, in two distinct foraminiferal assemblage zones respectively, and additionally brings up the fact that the unique adaptability to sea ice cover of the planktonic *N. pachyderma* may enforce the high P/B ratio connection to perennial sea ice (Polyak et al. 2013). One reason that the P/B ratio may be used as a sea ice indicator in the Arctic, is that this ratio is influenced by food supply to the seafloor, which in turn is affected by surface productivity (Berger and Diester-Haass 1988). For the purpose of this study, the interpretation of this is that extensive perennial sea ice may limit surface productivity, meaning the benthic community may have a reduced food supply and therefore reduced foraminiferal abundances, while simultaneously

allowing the planktonic species *N. pachyderma* to thrive. Vice versa, during open surface conditions, benthic foraminifera may grow larger communities while abundances of the planktonic *N. pachyderma* are lowered due to unfavorable oceanic conditions and/or increased competition in the water column (Marzen et al. 2016).

2.3 Sea ice biomarker reconstructions at the Yermak Plateau

Kremer et al. (2018) has in recent years produced reconstructions of sea ice variability at the Yermak Plateau (core site 039-2) using modern sea ice proxy biomarkers including IP_{25}, in combination with phytoplankton biomarkers (PIP_{25}) and tri-unsaturated lipids (HB III). These are biochemical molecules associated with sea ice living diatoms, and so increase in their concentrations proximate sea ice conditions. They conclude that in the last 160 ka a general pattern of sea ice cover during glacial stages and less sea ice during interglacial stages cannot be applied to this area (039-2) at the Yermak Plateau. Their findings show a bit more complex variability, and they state the following interpretations based on their biomarker data:

- The eastern Yermak Plateau had periodical marginal sea ice conditions during glacial intervals, with formation of polynyas north of Svalbard and sea ice margins occurring nearby the site of 039-2.
- A highly dynamic MIS 6 with waxing and waning of the Svalbard Barents Sea Ice Sheet (SBIS) possibly temporarily covering the Yermak Plateau.
- Extensive but variable sea ice cover at the Yermak Plateau during interglacial stages.
- Maxima of biomarker fluxes occurs during deglaciation stages.
- Differences in sea ice variability between the western and eastern Yermak Plateau during the last 30 ka (MIS 2 & MIS 1) highlights regional influences like ice sheet extent and Atlantic Water inflow (Kremer et al. 2018).

2.4 Aim and research questions

The overall aim of this project is to compare mainly the P/B ratios, the relative abundances of a few foraminiferal categories (i.e. planktonic, calcareous benthic and agglutinated benthic foraminifera) and to lesser extent sediment bulk density data, to the biomarker-based sea ice reconstruction of core 039-2. Specifically, the main research question of this study is the following:

- Will the potentially high P/B ratios (meaning more planktonic than benthic foraminifera) generated from relative abundance counts on core 045-2 correlate in time with the expected sea ice cover expansions or perennial ice (high IP_{25}) cover during the last 160 ka as suggested by Kremer et al., and vice versa if low P/B values (meaning more benthic than planktonic foraminifera) correlate in time with less extensive sea, or seasonally ice free, ice cover (low IP_{25}) (Kremer et al. 2018).

3. Method

3.1 Foraminiferal identification and categorization

The size fraction of foraminifera plays an important role when estimating the relative abundances in a sample, and a balance between ease of identification and reaching a representative count had to be reached. Counting the >63 µm fraction is especially important in the polar regions, where foraminifera grow small, but the >125 µm fraction made identification faster and easier and is a good size fraction to compare with many other studies (Polyak et al. 2013) and was therefore decided to be the size fraction this study would focus on. As mentioned, the taxonomic identification was simplified to involve a few general categories: 1. Planktonic foraminifera *N. pachyderma* and *T. quinqueloba*; 2. calcareous benthic foraminifera; 3. agglutinated benthic foraminifera; and 4. ostracodes.

When identification on species level in the more diverse benthic group was possible, significant exceptions to the usual species found in the core would be noted. The different categories were distinguished mostly by the textural qualities of the foraminiferal tests. Across all categories, even fragments would be counted as a single individual, as it was not possible to know to which individual

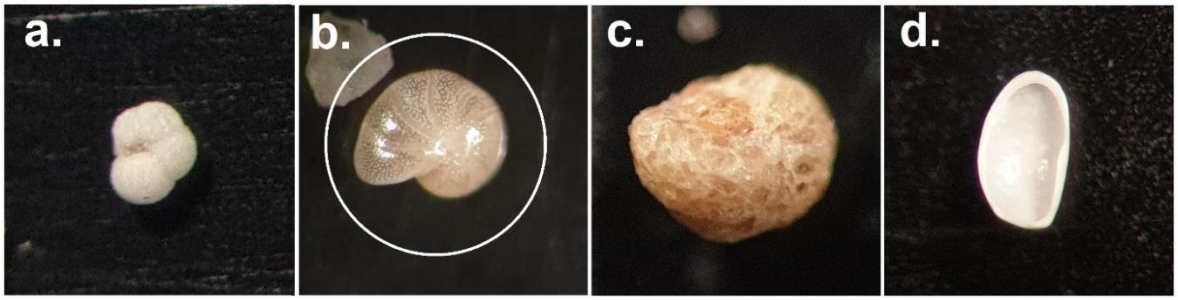

Figure 2: *A basic "identification scheme" of examples of the different categories:* ***a.*** *Planktonic foraminifera (N. pachyderma), T. quinqueloba looks somewhat similar, but differs in texture and generally are smaller;* ***b.*** *One example of a calcareous benthic foraminifera, recognizable by their different and more diverse morphology versus planktonics, and by their smoother texture and transluscent tests;* ***c.*** *An example of an agglutinated benthic foraminifera, recognizable by their texture of cemented grains;* ***d.*** *Ostracoda, recognizable by their thick non-chambered calcareous shells. Photos: Anton Almgren.*

the fragment belonged to or if it did not belong to a different individual at all and indeed constituted its own individual, and so on. In Figure 2 below is a diagram of examples from the different categories.

3.2 Counting

In the sample set of core 045-2 there were 120 vials of pre-prepared dried sediment, each representing 2 cm along the depth of the core, in 2 cm intervals, over 6 sections and approximately 5,25 meters of core. The sediment samples were prepared previous to this project by wet sieving over a >63 µm mesh sieve and then drying them.

One at the time, each sample was manually sieved through 125 µm aperture Retsch mesh sieves to remove the smaller fraction. The >125 µm fraction was then put on a gridded picking tray for counting. Identification was done through a Zeiss Stemi 2000 reflective light stereo microscope, and counting was done on the Android app Thing Counter (© 2012-2015, Kai Langenbach). In order for a relative abundance count in a sample to be termed statistically significant and quantitative the total count had to be at least 300 individuals (Lagoe 1977). A total count had to include *all* the material put onto the tray, doing this accounted for density-gravity sorting when the sieved material was transferred to the tray (i.e. denser material rolls out onto the picking tray first, potentially making the first 300 counts non-representative depending on how the material was spread out). Therefore, time consuming samples with an impractically large amount of material much greater than 300 counts, had to be split. Samples deemed too rich in foraminifera were split in half in an ASC Scientific MS-1 Microsplitter as many times as required to make the material manageable while still allowing for at least 300 counts. The number of half splits was documented on a spreadsheet to allow for upscaling to obtain total foraminiferal abundance numbers.

To avoid unwittingly counting the same material on the picking tray grid borders multiple times the convention conceptualized in Figure 3 below was devised:

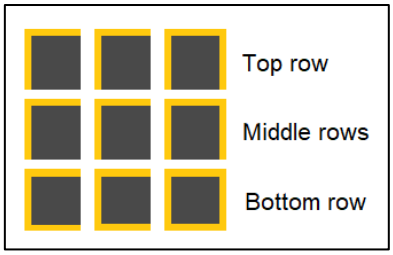

Figure 3: *A convention was set up to avoid counting anything on the picking tray grid borders repeatedly. Grid borders are gold and grid surfaces are black. Illustration: Anton Almgren.*

After a sample count was preformed all material was put back into the sample vial. The sieves, splitter and picking tray were manually decontaminated after each sample using compressed air and brushes to remove any remaining or stuck material. The sieves were cleaned using ultrasound in an Elma Elmasonic S 50 R when necessary. The core sample set had eight unavailable sample vials which could not be included in the data. In a number of samples, a number of *N. pachyderma* had been picked and removed from the sample vial for other projects, a decision was made to not include these due to lacking information about exactly how many had been picked and in which size fraction they were, instead this information is included as qualitative information. Furthermore, a number of *T. quinqueloba* at the top of the core were counted but were later suggested to be contamination (personal communication with supervisor Helen Coxall).

3.3 Data processing: 045-2

The counts, splitting information, estimated sample preservation quality and other notable findings were organized into a spreadsheet with already available data on sample net dry weight [g], core depth below seafloor (meters below seafloor) and core section information. Because a lot of samples were barren or had a foraminifer count of lower than 300, they were termed non-quantitative, while those with more than 300 were termed quantitative. Later, to bridge the gap between quantitative and non-quantitative counts, those samples with more than 100 counts were highlighted as "semi-quantitative". Core log data available at Stockholm University and a median age [ka] based on an age model from Gabriel West (West et al. 2019) was attached to each corresponding sample along the depth of the core (Appendix A).

The core log data consisted of sediment bulk density measurements along the core (provided by supervisor Matt O'Regan), this was added to the foraminiferal data in order to have a physical sediment property represented in the results. Since bulk density is a proxy for grain size, it will increase during glacial stages when sediment fluxes include larger grain sizes (personal communication with Matt O'Regan) and therefore it can be used as another discussion point when evaluating the results.

In a first step, the raw >125 µm foraminifera abundance data were consolidated into fewer more manageable taxonomic categories and adjusted for the half-splits where necessary. In a second step the >125 µm abundances were standardized per 1 gram of net dry sample weight (of the total material). A planktonic-to-benthic-ratio (P/B-ratio) for the entire core was acquired from the adjusted and standardized data with the following calculation in Equation 1:

$$P/B = \frac{no.\ planktonic\ taxa}{no.\ benthic\ taxa\ (agglutinated\ and\ calcareous)} \qquad \text{(Equation 1)}$$

All data available or generated for core 045-2 can be found in Appendix A.

3.4 Data processing: 039-2

For the sake of consistency, the age model used by (Kremer et al. 2018) in their PS92/039-2 study, was replaced with the 039-2 age model by Gabriel West (West et al. 2019). To further simplify it was decided to only use IP_{25} to represent the biomarker method. Specifically, IP_{25} / Sediment [g/cc] was plotted against age, and was decided to be representative, at least temporally of both IP_{25} measurements. The biomarker data was made available through the supplementary data link in Appendix A of Kremer et al. (2018). The data used in this study, along with the age model data can be found in Appendix B.

4. Results

4.1 P/B ratio and absolute abundances in the depth domain (mbsf)

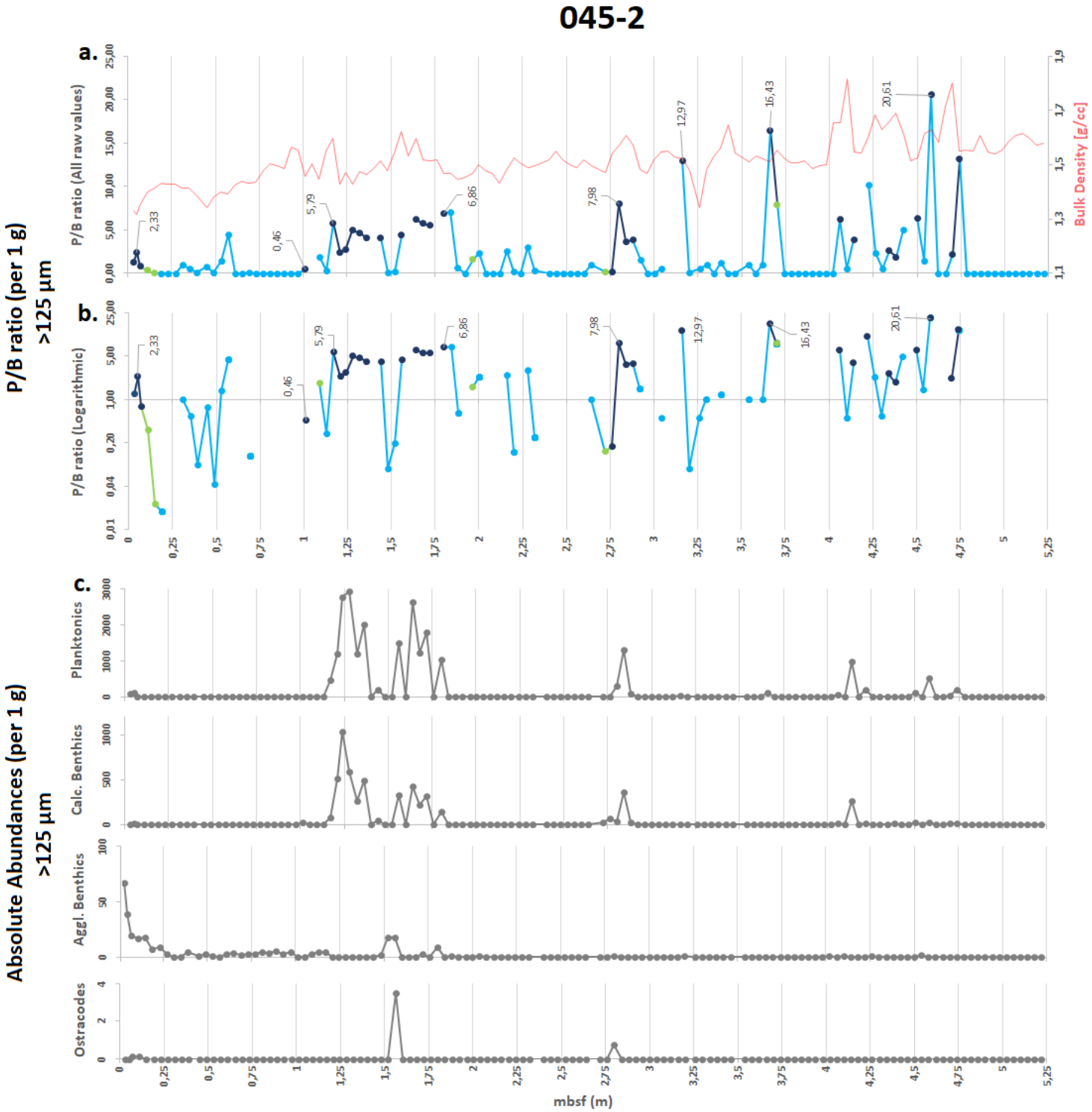

Figure 4: *Abundance data versus depth in core (meters below seafloor):* ***a.*** *P/B ratio from all raw data with quantitative samples in dark blue, "semi-quantitative" (>100 counts) in green, non-quantitative samples in light blue and sediment bulk density (provided by supervisor Matt O'Regan) in red;* ***b.*** *P/B ratio on a logarithmic scale with 0-values removed (cannot be plotted on log scale) and the same colour scheme as above;* ***c.*** *Four graphs plotting absolute abundances per 1 g for all the categories.*

The values in Figure 4 refers to P/B ratios and absolute abundances in core 045-2 only, plotted against mbsf depth (m). In Figure 4a the P/B ratio values (here plotted on a linear scale) cover the length of the core from about 0 mbsf to about 5,25 mbsf. Most values seem to be close to zero and non-quantitative (light blue). Large spikes occur throughout the length of the core, and the highest P/B ratio peaks occur in roughly the same interval (3,5 to 4,75 mbsf) as the bulk density peaks (>1,7 g/cc) here indicated by the red line.

In Figure 4b the P/B ratio (here plotted on a logarithmic scale) values that are 0 are not displayed as they cannot be defined, and therefore some values drop out. Especially after about 4,75 mbfs there are no defined values. However, all quantitative (dark blue) and "semi-quantitative" values (green) are preserved when moved onto the log scale. There are only three P/B ratio values dipping below 1 (1:1). These dips occur once close to the sea floor, once at 1,0 mbsf, and lastly again at 2,75 mbsf. Between 1,0 and 2,0 mbsf there is a cluster of quantitative P/B ratio values that seem to hover around a 5:1 ratio.

In Figure 4c the absolute abundances of foraminiferal counts are shown in relative to each other. In general, the absolute abundance fluxes seem to diminish downcore. It is obvious here again that most samples are non-quantitative or close to barren of foraminiferal material. The spikes in the different categories seem to move roughly synchronous along the depth of the core. One exception is the peak of agglutinated benthic foraminifera near the top of the core (0 to 0,25 mbsf) that is not mirrored in the other categories. Overall, planktonic foraminifera seem to show the highest absolute abundances often peaking close or above 1000 individuals per 1 g dry weight sediment, while calcareous benthic foraminifera generally fall below 500 individuals and only peaks 1000 individuals at about 1,25 mbsf.

4.2 P/B ratio, absolute abundances, bulk density and IP_{25} versus age

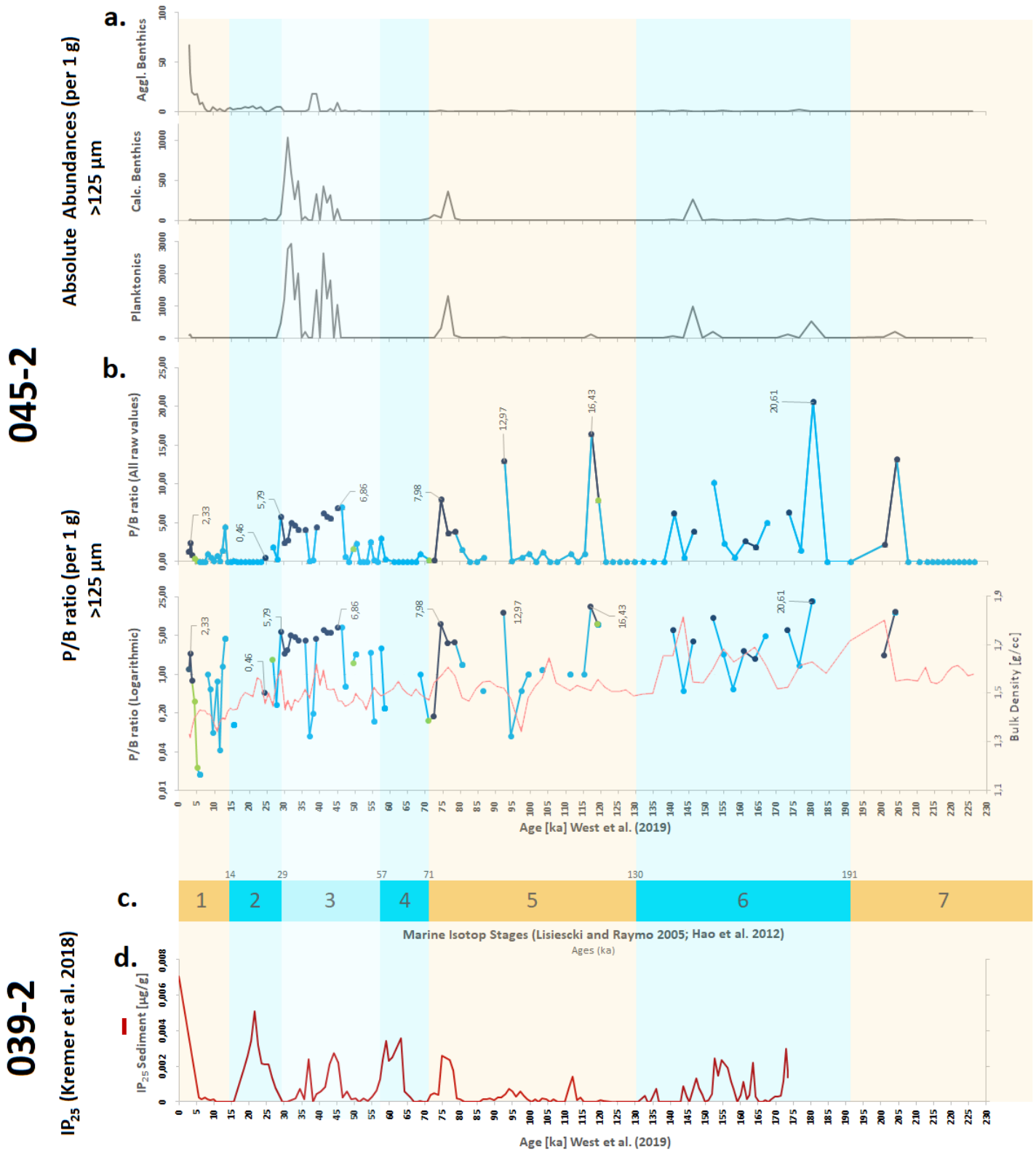

Figure 5: *Abundance data from core 045-2 along with IP_{25} biomarker data from core 039-2 (Kremer et al. 2018):* ***a.*** *Absolute abundances of the foraminiferal categories minus ostracodes;* ***b.*** *P/B ratios according to the same scheme as Figure 4, this time with bulk density (pale red line) transposed over the logarithmic chart ;* ***c.*** *Marine isotope stages, with yellow indicating interglacial stages and blue colors indicating glacial stages, the numbers in small font marks the boundaries in years BP [ka];* ***d.*** *IP_{25} biomarker data on the same timescale as the above charts.*

isotope stages (MIS 1 to MIS 7). The first thing to notice is that the age model for core 039-2 comprises a shorter timeframe of the Quaternary, only down to about 175 ka BP, while the age model for core 045-2 reaches down to about 227 ka BP. In Figure 5a the absolute abundances of all categories except ostracodes are here presented versus age [ka].

Figure 5b, 5c, and 5d presents a comparison between P/B ratios and bulk density aligned in time with the IP_{25} biomarker data from core 039-2 and a basic illustration of the most recent 7 marine isotope stages. A lot of variability is visible over time with the IP_{25} biomarker, but most higher peaks seem to align with glacial stages MIS 6 and MIS 2 to 4. A large biomarker flux is also noticeable at MIS 1. MIS 5 show only a few subdued fluxes. There is generally no direct alignment between IP_{25} peaks and P/B ratio peaks, only at about 75 ka BP does a biomarker spike correlate in time with a P/B spike. However, some general patterns common between IP_{25} and P/B ratios are observable. MIS 6 show large variations and a generally diminished signal toward the end of MIS 6 for both metrics. In MIS 5 the signals are mostly absent but shows roughly three coincidental or near coincidental spikes sporadically throughout the stage. P/B ratio data for MIS 2-4 is clustered around the latter half of MIS 3 which has a corresponding IP_{25} signal. A final, subdued P/B ratio cluster in MIS 1 corresponds to a very high peak in IP_{25}.

4.4 Additional qualitative findings (045-2)

Figure 6: *Additional findings from core 045-2:* ***a.*** *Possibly a Bulimina* sp. *found at about 2,8 mbsf (~75 ka), as well as at about 1,13 mbsf (28 ka);* ***b.*** *A pristine fossil of possibly a Quinqueloculina* sp. *Found at about 1,56 mbsf (~39 ka);* ***c.*** *Examples of relict burrow structures the were found throughout the core, especially through a sequence between 1,88 to 2,32 mbsf (47 to 59 ka);* ***d.*** *More burrow structure relicts in a light and a dark phase. Photos: Anton Almgren.*

Figure 6 shows examples of notable findings from core 045-2. Although these species and findings cannot be exactly and accurately identified that may be of interest in relation to the other results.

5. Discussion

Focusing on the result of quantitative data presented in figure 5, the hypothesis that a high P/B ratio (higher proportion of planktonic taxa) could indicate perennial sea ice conditions is supported by the results in the sense that most of the high P/B peaks seem to occur during marine isotope stages MIS 6 and MIS 2-4 which are considered to be largely glacial stages, and two out of three P/B ratio values below 1 occur during MIS 1 and MIS 5, which are considered to be largely interglacial stages, while one of the three P/B <1 values occur counter-hypothetically in the early half of MIS 2, a glacial stage. The sediment bulk density seems to mostly support the pattern of the P/B ratio and therefore further supporting the idea of higher P/B ratios during glacial stages. The spike in agglutinated benthic foraminifera absolute abundance in MIS 1 to present, and the contemporaneous lack of calcareous benthic foraminifera is a common feature in some regions of the modern Arctic Ocean, and since agglutinated benthic foraminifera may indicate seasonally ice free conditions (Cronin et al. 2008) this aligns well with the trends of MIS 1.

Putting the P/B ratios in relation to the interpretations by Kremer et al. of their biomarker data from core 039-2 (Kremer et al. 2018) makes it possible to support a couple of their conclusions about sea ice cover at the Yermak Plateau. First, the extremely variable P/B ratios during the glacial MIS 6 (Figure 5b) could perhaps support their interpretation of a highly dynamic MIS 6 with waxing and waning of the SBIS ice sheet and possible sea ice coverage of the Yermak Plateau, as the P/B highs correlate somewhat closely in time with IP_{25} highs, which are interpreted as an increase in sea ice living diatoms, and therefore sea ice. Secondly, extensive but variable sea ice during interglacial stages is a pattern that can be seen in the P/B ratios during the MIS 5 interglacial, especially toward late MIS 5 where a P/B spike correlates very close in time, around 70 to 80 ka BP, with a spike in increased IP_{25} flux.

The most continuous sequence of quantitative P/B ratio data occurs in the latter half of MIS 3 (~45 to 25 ka BP), which aligns pretty well with the fact that Kremer et al. associates the latter half of MIS 3 with severe sea ice above the Yermak Plateau, and proximity to a highly productive marginal ice zone. It is also along this sequence that there is a notable presence of different morphotypes of *N. pachyderma*, possibly *N. pachyderma* dex. and *N. pachyderma incompta*. There is also a spotting of a possible *Quinqueloculina* sp. and *Bulimina* sp. in this late mostly glacial MIS 3 sequence (Figure 6a and 6b for photo reference and Appendix A for data points) since these are not really found anywhere else in the core, their presence could be a clue to potentially special conditions during the mostly glacial MIS 3. Prior to this sequence, in the early half of MIS 3 there is a continuous presence of burrow structures between about 59 to 47 ka BP. These structures are spread out sporadically throughout the core and are mostly associated with sections barren of foraminifera. They occur as either dark or yellow phase tubes, flakes and smaller fragments. These burrow structures are interpreted as increased benthic activity, and therefore increased food supply to the seafloor, but their association with foraminifera is unclear, but this probably means that extreme carbonate dissolution has occurred, erasing almost all calcareous fossils (Figure 6c and 6d for photo reference and Appendix A for data points).

There is indeed more information to be gathered in this core than rough relative foraminiferal abundances and P/B ratios. A more thorough taxonomic abundance count of core 045-2 could potentially give more detailed and varied information about the past sea ice conditions above the Yermak Plateau. At the very least, the conclusion made by Kremer et al. that the history of sea ice extent at the Yermak Plateau is not straightforward can be observed in the P/B ratios.

Because of some major insecurities in the method, including unaccountability of potential selective dissolution and fragmentation of foraminifera, omission of the >63 µm size fraction, unaccountability of planktonic foraminifers picked and removed from the sample set, as well as the low amount of quantitative counts and fully quantitative data points this study cannot confidently neither support nor discard the P/B ratio as a useful tool in determining past sea ice conditions in the Arctic.

6. Conclusion

In conclusion, while the foraminiferal P/B ratio in marine sediments is widely regarded and used as a relatively easily obtainable metric associated with sea ice conditions, when taking several uncertainties associated with method and execution this study cannot confidently say that high P/B ratios correlate

in time with glacial stages, and low P/B ratios with interglacial stages/seasonally ice free conditions. Although some general common patterns can be observed between the P/B ratio and biomarker data, which means this metric also cannot be discarded. Before fully embracing P/B ratio as a kind of sea ice proxy for the Yermak Plateau, a statistically significant correlation between the ratios and other sea ice proxies should be reached. Furthermore, core 045-2 holds a lot more information than this study is able present, abundance counts on the taxonomic level could probably reveal more information about the past sea ice extent above the Yermak Plateau.

Acknowledgements

I would like to express my sincerest gratitude to my supervisors Helen Coxall and Matt O'Regan for organizing this project, providing me with material, as well as for their guidance and support. In the middle of an outbreak of a pandemic their effort to support me has been all the more invaluable. I would also like to thank Gabriel West for his advice and for instructing me on lab equipment and the sieving procedure. Last, but not least a big thank you to my course mates for their support and company.

The sediment cores used and referenced in this project were cored by staff of Expedition PS92 of R/V POLARSTERN. Dry sediment samples and core log data was provided by my supervisors at the Department of Geological Sciences at Stockholm University.

References

Arrigo, Kevin R., and Gert L. van Dijken. 2015. 'Continued Increases in Arctic Ocean Primary Production'. *Progress in Oceanography*, Synthesis of Arctic Research (SOAR), 136 (August): 60–70. https://doi.org/10.1016/j.pocean.2015.05.002.

Berger, W. H, and L Diester-Haass. 1988. 'Paleoproductivity: The Benthic/Planktonic Ratio in Foraminifera as a Productivity Index'. *Marine Geology* 81 (1): 15–25. https://doi.org/10.1016/0025-3227(88)90014-X.

Chauhan, T., T. L. Rasmussen, R. Noormets, M. Jakobsson, and K. A. Hogan. 2014. 'Glacial History and Paleoceanography of the Southern Yermak Plateau since 132 Ka BP'. *Quaternary Science Reviews*, APEX II: Arctic Palaeoclimate and its Extremes, 92 (May): 155–69. https://doi.org/10.1016/j.quascirev.2013.10.023.

Cronin, Thomas M., Shannon A. Smith, Frédérique Eynaud, Matthew O'Regan, and John King. 2008. 'Quaternary Paleoceanography of the Central Arctic Based on Integrated Ocean Drilling Program Arctic Coring Expedition 302 Foraminiferal Assemblages'. *Paleoceanography* 23 (1). https://doi.org/10.1029/2007PA001484.

Cusset, Fanny, Jérôme Fort, Mark Mallory, Birgit Braune, Philippe Massicotte, and Guillaume Massé. 2019. 'Arctic Seabirds and Shrinking Sea Ice: Egg Analyses Reveal the Importance of Ice-Derived Resources'. *Scientific Reports* 9 (1): 15405. https://doi.org/10.1038/s41598-019-51788-4.

Geissler, W. H., W. Jokat, and H. Brekke. 2011. 'The Yermak Plateau in the Arctic Ocean in the Light of Reflection Seismic Data-Implication for Its Tectonic and Sedimentary Evolution'. *Geophysical Journal International* 187 (3): 1334–62. https://doi.org/10.1111/j.1365-246X.2011.05197.x.

Hao, Qingzhen, Luo Wang, Frank Oldfield, Shuzhen Peng, Li Qin, Yang Song, Bing Xu, Yansong Qiao, Jan Bloemendal, and Zhengtang Guo. 2012. 'Delayed Build-up of Arctic Ice Sheets during 400,000-Year Minima in Insolation Variability'. *Nature* 490 (7420): 393–96. https://doi.org/10.1038/nature11493.

Husum, Katrine, Morten Hald, Ruediger Stein, and Monika Weißschnur. 2015. 'Recent Benthic Foraminifera in the Arctic Ocean and Kara Sea Continental Margin'. *Arktos* 1 (1): 5. https://doi.org/10.1007/s41063-015-0005-9.

Ingólfsson, Ólafur, and Jon Y. Landvik. 2013. 'The Svalbard–Barents Sea Ice-Sheet – Historical, Current and Future Perspectives'. *Quaternary Science Reviews* 64 (March): 33–60. https://doi.org/10.1016/j.quascirev.2012.11.034.

Jakobsson, Martin, Johan Nilsson, Leif Anderson, Jan Backman, Göran Björk, Thomas M. Cronin, Nina Kirchner, et al. 2016. 'Evidence for an Ice Shelf Covering the Central Arctic Ocean during the Penultimate Glaciation'. *Nature Communications* 7 (1): 10365. https://doi.org/10.1038/ncomms10365.

Kashiwase, Haruhiko, Kay I. Ohshima, Sohey Nihashi, and Hajo Eicken. 2017. 'Evidence for Ice-Ocean Albedo Feedback in the Arctic Ocean Shifting to a Seasonal Ice Zone'. *Scientific Reports* 7 (1): 8170. https://doi.org/10.1038/s41598-017-08467-z.

Klenke, Martin, and Hans Werner Schenke. 2002. 'A New Bathymetric Model for the Central Fram Strait'. *Marine Geophysical Researches* 23 (4): 367–78. https://doi.org/10.1023/A:1025764206736.

Kremer, Anne, Rüdiger Stein, Kirsten Fahl, Z. Yang, Z. Ji, S. Wiers, Jens Matthiessen, et al. 2018. 'Changes in Sea Ice Cover and Ice Sheet Extent at the Yermak Plateau during the Last 160 Ka – Reconstructions from Biomarker Records'. *Quaternary Science Reviews* 182 (February): 93–108.

Lagoe, Martin B. 1977. 'Recent Benthic Foraminifera from the Central Arctic Ocean'. *Journal of Foraminiferal Research* 7 (2): 106–29. https://doi.org/10.2113/gsjfr.7.2.106.

Lisiecki, Lorraine E., and Maureen E. Raymo. 2005. 'A Pliocene-Pleistocene Stack of 57 Globally Distributed Benthic Δ18O Records'. *Paleoceanography* 20 (1). https://doi.org/10.1029/2004PA001071.

Martin, T., and P. Wadhams. 1999. 'Sea-Ice Flux in the East Greenland Current'. *Deep Sea Research Part II: Topical Studies in Oceanography* 46 (6): 1063–82. https://doi.org/10.1016/S0967-0645(99)00016-8.

Marzen, Rachel E., Lauren H. DeNinno, and Thomas M. Cronin. 2016. 'Calcareous Microfossil-Based Orbital Cyclostratigraphy in the Arctic Ocean'. *Quaternary Science Reviews* 149 (October): 109–21. https://doi.org/10.1016/j.quascirev.2016.07.004.

'National Snow and Ice Data Center |'. n.d. Accessed 20 May 2020. https://nsidc.org/.

Nilsen, Frank, Ragnheid Skogseth, Juni Vaardal-Lunde, and Mark Inall. 2016. 'A Simple Shelf Circulation Model: Intrusion of Atlantic Water on the West Spitsbergen Shelf'. *Journal of Physical Oceanography*, 2016.

Notz, Dirk, and Julienne Stroeve. 2018. 'The Trajectory Towards a Seasonally Ice-Free Arctic Ocean'. *Current Climate Change Reports* 4 (4): 407–16. https://doi.org/10.1007/s40641-018-0113-2.

Osborne, Emily, Thomas Cronin, and Jesse Farmer. 2017. 'Paleoceanographic Perspectives on Arctic Ocean Change', December.

Peeken, Ilka. 2016. ‘The Expedition PS92 of the Research Vessel POLARSTERN to the Arctic Ocean in 2015’. Berichte zur Polar- und Meeresforschung. Berichte Zur Polar- Und Meeresforschung = Reports on Polar and Marine Research. Bremerhaven: Alfred Wegener Institute for Polar and Marine Research. 2 February 2016.

Polyak, Leonid, Richard B. Alley, John T. Andrews, Julie Brigham-Grette, Thomas M. Cronin, Dennis A. Darby, Arthur S. Dyke, et al. 2010. ‘History of Sea Ice in the Arctic’. *Quaternary Science Reviews*, Special Theme: Arctic Palaeoclimate Synthesis (PP. 1674-1790), 29 (15): 1757–78. https://doi.org/10.1016/j.quascirev.2010.02.010.

Polyak, Leonid, Kelly M. Best, Kevin A. Crawford, Edward A. Council, and Guillaume St-Onge. 2013. ‘Quaternary History of Sea Ice in the Western Arctic Ocean Based on Foraminifera’. *Quaternary Science Reviews*, Sea Ice in the Paleoclimate System: the Challenge of Reconstructing Sea Ice from Proxies, 79 (November): 145–56. https://doi.org/10.1016/j.quascirev.2012.12.018.

Rashid, Harunur, Leonid Polyak, and Ellen Mosley-Thompson. 2011. *Abrupt Climate Change: Mechanisms, Patterns, and Impacts*. Washington, UNITED STATES: American Geophysical Union. http://ebookcentral.proquest.com/lib/sub/detail.action?docID=1184588.

Schell, Trecia M., David B. Scott, André Rochon, and Steve Blasco. 2008. ‘Late Quaternary Paleoceanography and Paleo-Sea Ice Conditions in the Mackenzie Trough and Canyon, Beaufort SeaThis Article Is One of a Series of Papers Published in This Special Issue on the Theme *Polar Climate Stability Network* .’ Edited by Pete Hollings. *Canadian Journal of Earth Sciences* 45 (11): 1399–1415. https://doi.org/10.1139/E08-054.

Scott, D. B., and G. Vilks. 1991. ‘Benthic Foraminifera in the Surface Sediments of the Deep-Sea Arctic Ocean’. *Journal of Foraminiferal Research* 21 (1): 20–38. https://doi.org/10.2113/gsjfr.21.1.20.

Spielhagen, Robert F., Kirstin Werner, Steffen Aagaard Sørensen, Katarzyna Zamelczyk, Evguenia Kandiano, Gereon Budeus, Katrine Husum, Thomas M. Marchitto, and Morten Hald. 2011. ‘Enhanced Modern Heat Transfer to the Arctic by Warm Atlantic Water’. *Science* 331 (6016): 450–53.

Stein, R. 2008. ‘Chapter Four Proxies Used for Palaeoenvironmental Reconstructions in the Arctic Ocean’. In *Developments in Marine Geology*, 2:133–243. Elsevier. https://doi.org/10.1016/S1572-5480(08)00004-3.

Stein, Ruediger, Kirsten Fahl, Inka Schade, Adelina Manerung, Saskia Wassmuth, Frank Niessen, and Seung-Il Nam. 2017. ‘Holocene Variability in Sea Ice Cover, Primary Production, and Pacific-Water Inflow and Climate Change in the Chukchi and East Siberian Seas (Arctic Ocean)’. *JOURNAL OF QUATERNARY SCIENCE* 32 (3): 362–79. https://doi.org/10.1002/jqs.2929.

West, Gabriel, Darrell Kaufman, F. Muschitiello, Matthias Forwick, Jens Matthiessen, Jutta Wollenburg, and Matt O'Regan. 2019. ‘Amino Acid Racemization in Quaternary Foraminifera from the Yermak Plateau, Arctic Ocean’. *Geochronology* 1 (November): 53–67. https://doi.org/10.5194/gchron-1-53-2019.

Wetmore, Karen. 1996. ‘Foram Facts An Introduction to Foraminifera’. *The Paleontological Society Papers* 2 (October): 227–30. https://doi.org/10.1017/S1089332600003296.

Zheng, Jianqiu, Qiong Zhang, Qiang Li, Qiang Zhang, and Ming Cai. 2019. ‘Contribution of Sea Ice Albedo and Insulation Effects to Arctic Amplification in the EC-Earth Pliocene Simulation’. *Climate of the Past* 15 (1): 291–305. https://doi.org/10.5194/cp-15-291-2019.

Appendix A: 045-2 data

PS92/045-2

Core and sample information									Total counts unadjusted (>125 µm)							Qualitative information (>125 µm) Significant presence of:					
Section	Net dry weight [g]	Preservation quality	Half splits (>125 µm fraction)	Bot [cm]	Top [cm]	Mid-Depth (mbsf) [m]	Median age [ka] *(West et al. 2019)*	Bulk Density [g/cc]	Planktonic foraminifera (*N. Pachyderma*)	Planktonic fragments (*N. pachyderma*)	T. Quinqueloba (contamination)	Calcareous benthics	Agglutinated benthics	Ostracodes	Total count	Picked *N. pachyderma* missing: Yes(number of)	Different *N. pachyderma* morphotype	Sponge spicule fragments	Burrow structures	Dissolution	Uncommon species
1	7,3	moderate	2	2	4	0,03	3,0	1,3292	141	26	15	14	124	0	320	Y (~40)					
1	8,6	poor-moderate	2	4	6	0,05	3,4	1,3163	219	54	0	34	83	0	390			spicules			
1	7,5	poor-moderate	0	6	8	0,07	3,8	1,3549	107	42	1	43	148	1	342	Y (50)					
1	8,5	poor-moderate	0	10	12	0,11	4,6	1,3975	30	21	0	15	144	1	211	Y (?)					
1	8,3	poor-moderate	0	14	16	0,15	5,3	1,4147	2	1	0	2	144	0	149			spicules			
1	8,7	poor	0	18	20	0,19	6,1	1,4313	1	0	0	0	63	0	64						
1	7,9	poor-moderate	0	22	24	0,23	6,8	1,4286	0	0	0	0	72	0	72						
1	7,9	poor	0	26	28	0,27	7,6	1,4284	0	0	0	0	26	0	26			spicules			
1	7,8	poor	0	30	32	0,31	8,3	1,4146	2	1	0	2	1	0	6						
1	8,0	poor	0	34	36	0,35	9,1	1,4143	6	7	0	20	4	0	37						
1	8,0	poor	0	38	40	0,39	9,9	1,3865	2	1	0	0	34	0	37						
2	5,2	poor	0	4	6	0,45	11,0	1,3423	3	3	0	1	7	0	14						
2	8,3	poor	0	8	10	0,49	11,8	1,3817	1	0	0	0	23	0	24						
2	8,0	good	0	12	14	0,53	12,5	1,4003	15	2	0	5	7	0	29						
2	7,4	good	0	16	18	0,57	13,3	1,3906	21	6	0	4	2	0	33						
2	7,5	very poor	0	20	22	0,61	14,0	1,4236	0	0	0	0	23	0	23						
2	8,7	poor	0	24	26	0,65	14,8	1,437	0	0	0	0	32	0	32		N.p morph				
2	8,3	poor	0	28	30	0,69	15,6	1,43	2	0	0	0	16	0	18						
2	7,6	poor	1	32	34	0,73	16,6	1,4355	0	0	0	0	10	0	10						
2	9,6	poor	2	36	38	0,77	17,8	1,4794	0	0	0	0	7	0	7						
2	10,3	poor	2	40	42	0,81	18,9	1,5018	0	0	0	0	12	0	12						
2	9,7	poor	1	44	46	0,85	20,0	1,4965	0	0	0	0	20	0	20						
2	9,9	poor	1	48	50	0,89	21,2	1,4868	0	0	0	0	27	0	27						
2	11,4	poor	1	52	54	0,93	22,3	1,5627	0	0	0	1	15	0	16						
2	7,3	poor	2	56	58	0,97	23,4	1,5528	0	0	0	0	8	0	8						
2	9,6	very good	0	60	62	1,01	24,6	1,4562	84	25	0	238	0	0	347	Y (~40)					
2	9,0	UNAVAILABLE		64	66	1,05	25,7	1,5023	UNAVAILABLE						UNAVAILABLE						
2	12,0	very good	0	68	70	1,09	26,8	1,4464	96	6	2	26	30	0	160	Y (~30)	N.p morph				
2	10,8	moderate	1	72	74	1,13	28,0	1,5495	7	2	0	9	23	0	41			spicules			*Bulimina* sp
2	9,5	moderate-good	3	76	78	1,17	29,1	1,5961	408	142	0	89	6	0	645	Y (~40)	N.p morph				
2	5,5	moderate-good	4	80	82	1,21	30,2	1,4296	361	53	0	178	0	0	592	Y (19)	N.p morph				
3	10,2	moderate-good	6	0	2	1,24	31,0	1,4695	388	53	0	165	0	0	606	Y (20)	N.p morph				
3	9,6	moderate-good	6	4	6	1,28	32,1	1,4276	390	51	0	89	0	0	530	Y (20)	N.p morph				
3	9,3	moderate-good	5	8	10	1,32	33,1	1,4746	324	28	0	76	0	0	428	Y (19)	N.p morph				
3	9,7	moderate	6	12	14	1,36	34,1	1,4639	261	44	0	75	0	0	380	Y (19)	N.p morph				
3	9,9	UNAVAILABLE		16	18	1,4	35,1	1,4837	UNAVAILABLE						UNAVAILABLE						
3	9,7	poor	2	20	22	1,44	36,1	1,5157	310	145	0	112	0	0	567						
3	9,9	poor	1	24	26	1,48	37,2	1,478	1	0	0	1	12	0	14						
3	10,1	poor	2	28	30	1,52	38,2	1,5425	9	0	0	0	45	0	54						
3	9,1	moderate	5	32	34	1,56	39,2	1,6206	406	16	0	92	5	1	520	Y (16)	N.p morph				*Quinqueloculina*
3	11,5	UNAVAILABLE		36	38	1,6	40,2	1,5316	UNAVAILABLE						UNAVAILABLE						
3	9,8	good	6	40	42	1,64	41,3	1,5969	357	47	0	65	0	0	469	Y (14)	N.p morph				
3	9,9	good	5	44	46	1,68	42,3	1,5183	330	52	0	67	0	0	449	Y (18)	N.p morph				
3	10,3	moderate-good	5	48	50	1,72	43,3	1,5148	474	106	0	104	1	0	685	Y (17)					
3	8,9	UNAVAILABLE		52	54	1,76	44,3	1,5177	UNAVAILABLE						UNAVAILABLE						

3	7,0	moderate-good	4	56	58	1,8	45,3	1,4662	355	98	0	62	4	0	519	Y (25)			
3	8,6	moderate	0	60	62	1,84	46,4	1,4672	12	9	0	1	2	0	24				
3	8,5	poor	0	64	66	1,88	47,4	1,4442	4	2	0	2	8	0	16			burrows	
3	9,0	poor	0	68	70	1,92	48,4	1,4533	0	0	0	0	4	0	4			burrows	
3	9,1	poor	0	73	74	1,97	49,7	1,4684	25	43	0	40	3	0	111			burrows	
3	8,8	poor	0	76	78	2	50,5	1,498	3	11	0	1	5	0	20				
3	5,0	poor	0	80	82	2,04	51,5	1,4791	0	0	0	0	5	0	5			burrows	
3	9,0	poor	0	84	86	2,08	52,5	1,4688	0	0	0	0	3	0	3			burrows	
3	8,2	poor	0	88	90	2,12	53,5	1,4317	0	0	0	0	1	0	1			burrows	
3	9,2	good	0	92	94	2,16	54,5	1,4862	5	0	0	2	0	0	7			burrows	
3	12,2	good	0	96	98	2,2	55,6	1,5232	1	0	0	0	7	0	8			burrows	
4	11,6	poor	0	0	2	2,24	56,6	1,5017	0	0	0	0	2	0	2			burrows	
4	10,2	poor	0	4	6	2,28	57,6	1,4882	0	3	0	1	0	0	4			burrows	
4	9,2	poor	0	8	10	2,32	58,7	1,4961	0	3	0	11	1	0	15			burrows	
4	10,7	poor	0	16	18	2,4	61,2	1,5176	0	0	0	0	3	0	3				
4	11,1	poor	0	20	22	2,44	62,5	1,5502	0	0	0	0	3	0	3				
4	9,6	poor	0	24	26	2,48	63,7	1,5163	0	0	0	0	2	0	2				
4	10,3	poor	0	28	30	2,52	65,0	1,4995	0	0	0	0	3	0	3				
4	10,2	poor	0	32	34	2,56	66,2	1,4887	0		0	0	4	0	4				
4	9,9	barren	0	36	38	2,6	67,5	1,5181	0	0	0	0	0	0	0				
4	8,7	barren	0	40	42	2,64	68,7	1,4968	0	1	0	1	0	0	2			burrows	
4	8,2	good	0	48	50	2,72	71,3	1,47	11	14	0	171	2	0	198				
4	11,3	poor	1	52	54	2,76	72,7	1,5414	33	36	0	394	0	0	463	Y (~40)			
4	10,8	moderate-good	3	56	58	2,8	74,7	1,5713	380	35	0	50	2	1	468	Y (21)	N.p morph		*Bulimina* sp
4	12,6	good	6	60	62	2,84	76,7	1,6073	233	27	0	71	0	0	331				
4	9,0	good	1	64	66	2,88	78,6	1,5706	362	32	0	103	0	0	497	Y (23)			
4	9,8	good	0	68	70	2,92	80,6	1,4807	18	6	0	16	0	0	40				
4	9,5	good	0	72	74	2,96	82,6	1,4679	3	0	0	0	0	0	3				
4	10,4	poor	0	76	78	3	84,6	1,5184	0	0	0	0	2	0	2				
4	10,6	poor	0	80	82	3,04	86,6	1,5453	0	1	0	0	2	0	3				
4	9,3	UNAVAILABLE		84	86	3,08	88,6	1,5486	UNAVAILABLE						UNAVAILABLE				
4	11,6	UNAVAILABLE		88	90	3,12	90,6	1,5286	UNAVAILABLE						UNAVAILABLE				
4	9,4	moderate	0	92	94	3,16	92,6	1,5201	241	135	0	28	1	0	405				
4	11,0	poor	0	96	98	3,2	94,6	1,4764	1	0	0	0	13	0	14				
5	11,2	poor	0	0	2	3,26	97,5	1,3414	1	0	0	0	2	0	3			burrows	
5	10,4	poor	0	4	6	3,3	99,5	1,4822	0	1	0	0	1	0	2				
5	9,6	poor	0	8	10	3,34	101,5	1,5293	0	0	0	0	2	0	2			burrows	
5	10,8	poor	0	12	14	3,38	103,5	1,5616	14	30	0	33	3	0	80				
5	10,8	poor	0	16	18	3,42	105,5	1,6457	0	0	0	0	6	0	6				
5	8,9	barren	0	20	22	3,46	107,5	1,5422	0	0	0	0	0	0	0				
5	8,8	good	0	28	30	3,54	111,4	1,5118	1	0	0	0	1	0	1				
5	9,2	barren	0	32	34	3,58	113,4	1,5307	0	0	0	0	0	0	0				
5	8,6	good	0	36	38	3,62	115,4	1,5216	1	0	0	0	1	0	2				
5	8,4	moderate-good	1	40	42	3,66	117,4	1,5112	354	106	0	28	0	0	488				
5	8,9	moderate	0	44	46	3,7	119,4	1,5554	53	42	0	11	1	0	107				
5	8,0	poor	0	48	50	3,74	121,3	1,5242	0	0	0	0	1	0	1				
5	8,8	good	0	52	54	3,78	123,3	1,5082	1	0	0	0	0	0	1				
5	6,5	poor	0	56	58	3,82	125,3	1,5072	0	0	0	0	2	0	2				
5	8,9	barren	0	60	62	3,86	127,4	1,5135	0	0	0	0	0	0	0				
5	9,7	poor	0	64	66	3,9	129,5	1,4871	2	3	0	0	0	0	5				
5	10,6	barren	0	68	70	3,94	132,0	1,4968	0	0	0	0	0	0	0				
5	10,5	poor	0	72	74	3,98	134,9	1,5004	0	0	0	1	0	0	1				dissolution
5	11,2	poor	2	76	78	4,02	137,9	1,6531	0	0	0	0	4	0	4				
5	15,1	good	1	80	82	4,06	140,8	1,6551	443	38	0	75	3	0	559	Y (22)			
5	13,5	poor	3	84	86	4,1	143,7	1,8154	0	1	0	0	2	0	3				
5	10,5	good	5	88	90	4,14	146,5	1,5474	284	43	0	85	0	0	412	Y (17)			
5	11,0	UNAVAILABLE		92	94	4,18	149,3	1,5433	UNAVAILABLE						UNAVAILABLE				
5	11,2	poor	2	96	98	4,22	152,2	1,6007	328	225	0	54	0	0	607	Y (30)			
6	14,2	good	4	0	2	4,26	155,1	1,6846	7	0	0	2	1	0	10				
6	15,3	good	0	4	6	4,3	158,0	1,6298	14	2	0	27	2	0	45				
6	15,4	good	0	8	10	4,34	161,0	1,6579	233	51	0	109	1	0	394				
6	12,4	poor	0	12	14	4,38	164,1	1,6905	75	147	0	118	1	0	341				
6	12,9	poor	2	16	18	4,42	167,1	1,6129	19	21	0	8	0	0	48				
6	12,0	UNAVAILABLE		20	22	4,46	170,3	1,5158							UNAVAILABLE				
6	11,7	good	2	24	26	4,5	173,5	1,5262	297	78	0	58	1	0	434	Y (21)			
6	12,0	good	2	28	30	4,54	176,7	1,6134	8	2	0	0	7	0	17				
6	11,2	very good	4	32	34	4,58	180,3	1,6279	323	48	0	18	0	0	389	Y (17)			
6	15,2	barren	4	36	38	4,62	184,3	1,583	0	0	0	0	0	0	0				
6	16,2	barren	5	40	42	4,66	191,0	1,7149	0	0	0	0	0	0	0				
6	10,7	moderate	0	44	46	4,7	200,8	1,8001	262	53	0	143	0	0	458				dissolution
6	10,7	moderate-good	2	48	50	4,74	204,1	1,5502	453	114	0	43	0	0	610	Y (31)			
6	10,4	barren	0	52	54	4,78	207,2	1,5553	1	0	0	0	0	0	1				
6	4,1	barren	0	56	58	4,82	210,4	1,55	0	0	0	0	0	0	0				
6	11,9	barren	0	60	62	4,86	212,6	1,6066	2	1	0	0	0	0	3				
6	9,3	barren	0	64	66	4,9	214,1	1,5468	0	0	0	0	0	0	0				
6	11,2	barren	0	68	70	4,94	215,7	1,5399	0	0	0	0	0	0	0				
6	11,4	barren	0	72	74	4,98	217,2	1,5531	0	0	0	0	0	0	0			burrows	
6	11,4	barren	0	76	78	5,02	218,7	1,5862	0	0	0	0	0	0	0			burrows	
6	12,5	barren	0	80	82	5,06	220,2	1,6086	0	0	0	0	0	0	0				
6	5,6	barren	0	84	86	5,1	221,7	1,616	0	0	0	0	0	0	0				
6	10,4	barren	0	88	90	5,14	223,1	1,5977	0	0	0	0	0	0	0				
6	10,9	barren	0	92	94	5,18	224,6	1,5712	0	0	0	0	0	0	0				
6	11,9	barren	0	96	98	5,22	226,1	1,58	0	0	0	0	0	0	0				

PS92/045-2

PROCESSED DATA OUTPUTS

Section	Net dry weight [g]	Half splits (>125 µm fraction)	Mid-Depth (mbsf) [m]	Median age [ka] (*Weset al. 2019*)	Bulk Density [g/cc]	Abundances adjusted for half splits (>125 µm)					Adjusted abundances per 1 g (>125 µm)					P/B ratios			
						Planktonic (*N. Pachyderma*)	Calcareous benthics	Agglutinated benthics	Ostracodes	Total count	Planktonic (*N. pachyderma*)	Calcareous benthics	Agglutinated benthics	Ostracodes	Total count	Planktonic foraminifera	Benthic foraminifera	P/B-ratio	Quantitative P/B-ratio
1	7,3	2	0,03	3,0	1,3292	668	56	496	0	1220	91	8	68	0	166	90,9	75,1	1,21	1,21
1	8,6	2	0,05	3,4	1,3163	1092	136	332	0	1560	127	16	39	0	181	127,0	54,4	2,33	2,33
1	7,5	0	0,07	3,8	1,3549	149	43	148	1	341	20	6	20	0	46	19,9	25,5	0,78	0,78
1	8,5	0	0,11	4,6	1,3975	51	15	144	1	211	6	2	17	0	25	6,0	18,8	0,32	-
1	8,3	0	0,15	5,3	1,4147	3	2	144	0	149	0	0	17	0	18	0,4	17,7	0,02	-
1	8,7	0	0,19	6,1	1,4313	1	0	63	0	64	0	0	7	0	7	0,1	7,3	0,02	-
1	7,9	0	0,23	6,8	1,4286	0	0	72	0	72	0	0	9	0	9	0,0	9,2	0,00	-
1	7,9	0	0,27	7,6	1,4284	0	0	26	0	26	0	0	3	0	3	0,0	3,3	0,00	-
1	7,8	0	0,31	8,3	1,4146	3	2	1	0	6	0	0	0	0	1	0,4	0,4	1,00	-
1	8,0	0	0,35	9,1	1,4143	13	20	4	0	37	2	2	0	0	5	1,6	3,0	0,54	-
1	8,0	0	0,39	9,9	1,3865	3	0	34	0	37	0	0	4	0	5	0,4	4,2	0,09	-
2	5,2	0	0,45	11,0	1,3423	6	1	7	0	14	1	0	1	0	3	1,2	1,5	0,75	-
2	8,3	0	0,49	11,8	1,3817	1	0	23	0	24	0	0	3	0	3	0,1	2,8	0,04	-
2	8,0	0	0,53	12,5	1,4003	17	5	7	0	29	2	1	1	0	4	2,1	1,5	1,42	-
2	7,4	0	0,57	13,3	1,3906	27	4	2	0	33	4	1	0	0	4	3,6	0,8	4,50	-
2	7,5	0	0,61	14,0	1,4236	0	0	23	0	23	0	0	3	0	3	0,0	3,1	0,00	-
2	8,7	0	0,65	14,8	1,437	0	0	32	0	32	0	0	4	0	4	0,0	3,7	0,00	-
2	8,3	0	0,69	15,6	1,43	2	0	16	0	18	0	0	2	0	2	0,2	1,9	0,13	-
2	7,6	1	0,73	16,6	1,4355	0	0	20	0	20	0	0	3	0	3	0,0	2,6	0,00	-
2	9,6	2	0,77	17,8	1,4794	0	0	28	0	28	0	0	3	0	3	0,0	2,9	0,00	-
2	10,3	2	0,81	18,9	1,5018	0	0	48	0	48	0	0	5	0	5	0,0	4,7	0,00	-
2	9,7	1	0,85	20,0	1,4965	0	0	40	0	40	0	0	4	0	4	0,0	4,1	0,00	-
2	9,9	1	0,89	21,2	1,4868	0	0	54	0	54	0	0	5	0	5	0,0	5,4	0,00	-
2	11,4	1	0,93	22,3	1,5627	0	2	30	0	32	0	0	3	0	3	0,0	2,8	0,00	-
2	7,3	2	0,97	23,4	1,5528	0	0	32	0	32	0	0	4	0	4	0,0	4,4	0,00	-
2	9,6	0	1,01	24,6	1,4562	109	238	0	0	347	11	25	0	0	36	11,3	24,7	0,46	0,46
2	9,0		1,05	25,7	1,5023	UNAVAILABLE					-	-	-	-	-	UNAVAILABLE		-	
2	12,0	0	1,09	26,8	1,4464	102	26	30	0	158	9	2	3	0	13	8,5	4,7	1,82	-
2	10,8	1	1,13	28,0	1,5495	18	18	46	0	82	2	2	4	0	8	1,7	5,9	0,28	-
2	9,5	3	1,17	29,1	1,5961	4400	712	48	0	5160	462	75	5	0	541	461,7	79,7	5,79	5,79
2	5,5	4	1,21	30,2	1,4296	6624	2848	0	0	9472	1197	514	0	0	1711	1196,5	514,5	2,33	2,33
3	10,2	6	1,24	31,0	1,4695	28224	10560	0	0	38784	2763	1034	0	0	3797	2763,3	1033,9	2,67	2,67
3	9,6	6	1,28	32,1	1,4276	28224	5696	0	0	33920	2942	594	0	0	3536	2942,1	593,8	4,96	4,96
3	9,3	5	1,32	33,1	1,4746	11264	2432	0	0	13696	1211	262	0	0	1473	1211,2	261,5	4,63	4,63
3	9,7	6	1,36	34,1	1,4639	19520	4800	0	0	24320	2011	494	0	0	2505	2010,9	494,5	4,07	4,07
3	9,9		1,4	35,1	1,4837	UNAVAILABLE					-	-	-	-	-	UNAVAILABLE		-	
3	9,7	2	1,44	36,1	1,5157	1820	448	0	0	2268	188	46	0	0	234	187,6	46,2	4,06	4,06
3	9,9	1	1,48	37,2	1,478	2	2	24	0	28	0	0	2	0	3	0,2	2,6	0,08	-
3	10,1	2	1,52	38,2	1,5425	36	0	180	0	216	4	0	18	0	21	3,6	17,8	0,20	-
3	9,1	5	1,56	39,2	1,6206	13504	2944	160	32	16640	1489	325	18	4	1834	1488,5	342,2	4,35	4,35
3	11,5		1,6	40,2	1,5316	UNAVAILABLE					-	-	-	-	-	UNAVAILABLE		-	
3	9,8	6	1,64	41,3	1,5969	25856	4160	0	0	30016	2626	422	0	0	3048	2625,5	422,4	6,22	6,22
3	9,9	5	1,68	42,3	1,5183	12224	2144	0	0	14368	1240	217	0	0	1457	1239,5	217,4	5,70	5,70
3	10,3	5	1,72	43,3	1,5148	18560	3328	32	0	21920	1797	322	3	0	2122	1796,9	325,3	5,52	5,52
3	8,9		1,76	44,3	1,5177	UNAVAILABLE					-	-	-	-	-	UNAVAILABLE		-	

3	7,0	4	1,8	45,3	1,4662	7248	992	64	0	8304	1030	141	9	0	1181	1030,4	150,1	6,86	6,86
3	8,6	0	1,84	46,4	1,4672	21	1	2	0	24	2	0	0	0	3	2,4	0,3	7,00	-
3	8,5	0	1,88	47,4	1,4442	6	2	8	0	16	1	0	1	0	2	0,7	1,2	0,60	-
3	9,0	0	1,92	48,4	1,4533	0	0	4	0	4	0	0	0	0	0	0,0	0,4	0,00	-
3	9,1	0	1,97	49,7	1,4684	68	40	3	0	111	7	4	0	0	12	7,5	4,7	1,58	-
3	8,8	0	2	50,5	1,498	14	1	5	0	20	2	0	1	0	2	1,6	0,7	2,33	-
3	5,0	0	2,04	51,5	1,4791	0	0	5	0	5	0	0	1	0	1	0,0	1,0	0,00	-
3	9,0	0	2,08	52,5	1,4688	0	0	3	0	3	0	0	0	0	0	0,0	0,3	0,00	-
3	8,2	0	2,12	53,5	1,4317	0	0	1	0	1	0	0	0	0	0	0,0	0,1	0,00	-
3	9,2	0	2,16	54,5	1,4862	5	2	0	0	7	1	0	0	0	1	0,5	0,2	2,50	-
3	12,2	0	2,2	55,6	1,5232	1	0	7	0	8	0	0	1	0	1	0,1	0,6	0,14	-
4	11,6	0	2,24	56,6	1,5017	0	0	2	0	2	0	0	0	0	0	0,0	0,2	0,00	-
4	10,2	0	2,28	57,6	1,4882	3	1	0	0	4	0	0	0	0	0	0,3	0,1	3,00	-
4	9,2	0	2,32	58,7	1,4961	3	11	1	0	15	0	1	0	0	2	0,3	1,3	0,25	-
4	10,7	0	2,4	61,2	1,5176	0	0	3	0	3	0	0	0	0	0	0,0	0,3	0,00	-
4	11,1	0	2,44	62,5	1,5502	0	0	3	0	3	0	0	0	0	0	0,0	0,3	0,00	-
4	9,6	0	2,48	63,7	1,5163	0	0	2	0	2	0	0	0	0	0	0,0	0,2	0,00	-
4	10,3	0	2,52	65,0	1,4995	0	0	3	0	3	0	0	0	0	0	0,0	0,3	0,00	-
4	10,2	0	2,56	66,2	1,4887	0	0	4	0	4	0	0	0	0	0	0,0	0,4	0,00	-
4	9,9	0	2,6	67,5	1,5181	0	0	0	0	0	0	0	0	0	0	0,0	0,0	-	-
4	8,7	0	2,64	68,7	1,4968	1	1	0	0	2	0	0	0	0	0	0,1	0,1	1,00	-
4	8,2	0	2,72	71,3	1,47	25	171	2	0	198	3	21	0	0	24	3,0	21,0	0,14	-
4	11,3	1	2,76	72,7	1,5414	138	788	0	0	926	12	70	0	0	82	12,2	69,8	0,18	0,18
4	10,8	3	2,8	74,7	1,5713	3320	400	16	8	3744	307	37	1	1	347	307,3	38,5	7,98	7,98
4	12,6	6	2,84	76,7	1,6073	16640	4544	0	0	21184	1318	360	0	0	1678	1317,8	359,9	3,66	3,66
4	9,0	1	2,88	78,6	1,5706	788	206	0	0	994	87	23	0	0	110	87,2	22,8	3,83	3,83
4	9,8	0	2,92	80,6	1,4807	24	16	0	0	40	2	2	0	0	4	2,4	1,6	1,50	-
4	9,5	0	2,96	82,6	1,4679	3	0	0	0	3	0	0	0	0	0	0,3	0,0	-	-
4	10,4	0	3	84,6	1,5184	0	0	2	0	2	0	0	0	0	0	0,0	0,2	0,00	-
4	10,6	0	3,04	86,6	1,5453	1	0	2	0	3	0	0	0	0	0	0,1	0,2	0,50	-
4	9,3		3,08	88,6	1,5486	-	-	-	-	-	-	-	-	-	-	UNAVAILABLE		-	
4	11,6		3,12	90,6	1,5286	-	-	-	-	-	-	-	-	-	-	UNAVAILABLE		-	
4	9,4	0	3,16	92,6	1,5201	376	28	1	0	405	40	3	0	0	43	40,1	3,1	12,97	12,97
4	11,0	0	3,2	94,6	1,4764	1	0	13	0	14	0	0	1	0	1	0,1	1,2	0,08	-
5	11,2	0	3,26	97,5	1,3414	1	0	2	0	3	0	0	0	0	0	0,1	0,2	0,50	-
5	10,4	0	3,3	99,5	1,4822	1	0	1	0	2	0	0	0	0	0	0,1	0,1	1,00	-
5	9,6	0	3,34	101,5	1,5293	0	0	2	0	2	0	0	0	0	0	0,0	0,2	0,00	-
5	10,8	0	3,38	103,5	1,5616	44	33	3	0	80	4	3	0	0	7	4,1	3,3	1,22	-
5	10,8	0	3,42	105,5	1,6457	0	0	6	0	6	0	0	1	0	1	0,0	0,6	0,00	-
5	8,9	0	3,46	107,5	1,5422	0	0	0	0	0	0	0	0	0	0	0,0	0,0	-	-
5	8,8	0	3,54	111,4	1,5118	1	0	1	0	2	0	0	0	0	0	0,1	0,1	1,00	-
5	9,2	0	3,58	113,4	1,5307	0	0	0	0	0	0	0	0	0	0	0,0	0,0	-	-
5	8,6	0	3,62	115,4	1,5216	1	0	1	0	2	0	0	0	0	0	0,1	0,1	1,00	-
5	8,4	1	3,66	117,4	1,5112	920	56	0	0	976	109	7	0	0	116	109,4	6,7	16,43	16,43
5	8,9	0	3,7	119,4	1,5554	95	11	1	0	107	11	1	0	0	12	10,7	1,4	7,92	7,92
5	8,0	0	3,74	121,3	1,5242	0	0	1	0	1	0	0	0	0	0	0,0	0,1	0,00	-
5	8,8	0	3,78	123,3	1,5082	1	0	0	0	1	0	0	0	0	0	0,1	0,0	-	-
5	6,5	0	3,82	125,3	1,5072	0	0	2	0	2	0	0	0	0	0	0,0	0,3	0,00	-
5	8,9	0	3,86	127,4	1,5135	0	0	0	0	0	0	0	0	0	0	0,0	0,0	-	-
5	9,7	0	3,9	129,5	1,4871	5	0	0	0	5	1	0	0	0	1	0,5	0,0	-	-
5	10,6	0	3,94	132,0	1,4968	0	0	0	0	0	0	0	0	0	0	0,0	0,0	-	-
5	10,5	0	3,98	134,9	1,5004	0	1	0	0	1	0	0	0	0	0	0,0	0,1	0,00	-
5	11,2	2	4,02	137,9	1,6531	0	0	16	0	16	0	0	1	0	1	0,0	1,4	0,00	-
5	15,1	1	4,06	140,8	1,6551	962	150	6	0	1118	64	10	0	0	74	63,5	10,3	6,17	6,17
5	13,5	3	4,1	143,7	1,8154	8	0	16	0	24	1	0	1	0	2	0,6	1,2	0,50	-
5	10,5	5	4,14	146,5	1,5474	10464	2720	0	0	13184	994	258	0	0	1253	994,4	258,5	3,85	3,85
5	11,0		4,18	149,3	1,5433	-	-	-	-	-	-	-	-	-	-	UNAVAILABLE		-	
5	11,2	2	4,22	152,2	1,6007	2212	216	0	0	2428	198	19	0	0	217	198,0	19,3	10,24	10,24
6	14,2	4	4,26	155,1	1,6846	112	32	16	0	160	8	2	1	0	11	7,9	3,4	2,33	-
6	15,3	0	4,3	158,0	1,6298	16	27	2	0	45	1	2	0	0	3	1,0	1,9	0,55	-
6	15,4	0	4,34	161,0	1,6579	284	109	1	0	394	18	7	0	0	26	18,5	7,1	2,58	2,58
6	12,4	0	4,38	164,1	1,6905	222	118	1	0	341	18	10	0	0	28	17,9	9,6	1,87	1,87
6	12,9	2	4,42	167,1	1,6129	160	32	0	0	192	12	2	0	0	15	12,4	2,5	5,00	-
6	12,0		4,46	170,3	1,5158	-	-	-	-	-	-	-	-	-	-	UNAVAILABLE		-	
6	11,7	2	4,5	173,5	1,5262	1500	232	4	0	1736	128	20	0	0	148	127,9	20,1	6,36	6,36
6	12,0	2	4,54	176,7	1,6134	40	0	28	0	68	3	0	2	0	6	3,3	2,3	1,43	-
6	11,2	4	4,58	180,3	1,6279	5936	288	0	0	6224	531	26	0	0	557	531,1	25,8	20,61	20,61
6	15,2	4	4,62	184,3	1,583	0	0	0	0	0	0	0	0	0	0	0,0	0,0	-	-
6	16,2	5	4,66	191,0	1,7149	0	0	0	0	0	0	0	0	0	0	0,0	0,0	-	-
6	10,7	0	4,7	200,8	1,8001	315	143	0	0	458	29	13	0	0	43	29,4	13,3	2,20	2,20
6	10,7	2	4,74	204,1	1,5502	2268	172	0	0	2440	212	16	0	0	228	211,5	16,0	13,19	13,19
6	10,4	0	4,78	207,2	1,5553	1	0	0	0	1	0	0	0	0	0	0,1	0,0	-	-
6	4,1	0	4,82	210,4	1,55	0	0	0	0	0	0	0	0	0	0	0,0	0,0	-	-
6	11,9	0	4,86	212,6	1,6066	3	0	0	0	3	0	0	0	0	0	0,3	0,0	-	-
6	9,3	0	4,9	214,1	1,5468	0	0	0	0	0	0	0	0	0	0	0,0	0,0	-	-
6	11,2	0	4,94	215,7	1,5399	0	0	0	0	0	0	0	0	0	0	0,0	0,0	-	-
6	11,4	0	4,98	217,2	1,5531	0	0	0	0	0	0	0	0	0	0	0,0	0,0	-	-
6	11,4	0	5,02	218,7	1,5862	0	0	0	0	0	0	0	0	0	0	0,0	0,0	-	-
6	12,5	0	5,06	220,2	1,6086	0	0	0	0	0	0	0	0	0	0	0,0	0,0	-	-
6	5,6	0	5,1	221,7	1,616	0	0	0	0	0	0	0	0	0	0	0,0	0,0	-	-
6	10,4	0	5,14	223,1	1,5977	0	0	0	0	0	0	0	0	0	0	0,0	0,0	-	-
6	10,9	0	5,18	224,6	1,5712	0	0	0	0	0	0	0	0	0	0	0,0	0,0	-	-
6	11,9	0	5,22	226,1	1,58	0	0	0	0	0	0	0	0	0	0	0,0	0,0	-	-

Appendix B: 039-2 data **(Appendix A of Kremer et al.)**

Depth [m]	Age (ka) (West et al. 2019)	IP_{25}/Sed [¬µg/g]	IP_{25}/TOC [¬µg/g]
0,005	0,09	0,007060892	0,749622198
0,155	5,59	0,000236736	0,036290367
0,205	6,45	0,000161743	0,024786623
0,255	7,31	0,000261258	0,036655794
0,305	8,15	0,00016316	0,025443416
0,355	9,00	0,000108876	0,01592446
0,405	9,83	0,000156572	0,0251442
0,455	10,66	0	0
0,505	11,47	0	0
0,605	13,10	0	0
0,655	13,90	0	0
0,705	14,71	0	0
0,755	15,56	0	0
0,905	18,47	0,001919342	0,225627341
0,955	19,47	0,002576491	0,316455822
1,015	20,67	0,003417388	0,39923724
1,055	21,46	0,005084864	0,406715754
1,105	22,47	0,003192229	0,387561864
1,155	23,47	0,002161293	0,324929386
1,205	24,49	0,002094553	0,311028429
1,255	25,49	0,002086713	0,34303319
1,305	26,50	0,001343833	0,199785827
1,355	27,51	0,000757575	0,145778073
1,405	28,53	0,000397146	0,10967501
1,455	29,56	0	0
1,505	30,77	0	0
1,605	33,21	0,000213478	0,063369782
1,655	34,42	0,000714009	0,208812571
1,705	35,64	0,000156514	0,032732738
1,755	36,86	0,002400489	0,414018626
1,805	38,07	0	0
1,855	39,29	0,000436739	0,095451336
1,905	40,50	0,000565056	0,132777906
1,955	41,72	0,000803513	0,16450328
2,005	42,93	0,002119987	0,362496994
2,055	44,15	0,002746089	0,460854128
2,105	45,36	0,002178697	0,395548376
2,155	46,59	0,000234452	0,046446348
2,205	47,80	0,000603456	0,133423358
2,255	49,03	0,000158073	0,036154616
2,305	50,24	0,000190923	0,042334058
2,355	51,44	0	0
2,405	52,65	0,000188084	0,042665687
2,455	53,87	0,000054241	0,011101339
2,505	55,08	0,000269213	0,055569517
2,555	56,27	0,000645465	0,103946502
2,605	57,19	0,001281509	0,169585961
2,655	58,07	0,002326294	0,280061641
2,705	58,95	0,003452099	0,310397571
2,755	59,83	0,002305338	0,198936144
2,805	60,71	0,002496721	0,223231888
2,955	63,36	0,003589099	0,272557469
3,005	64,24	0,000562077	0,104450405
3,055	65,14	0,000363233	0,09208633
3,105	66,04	0,000233831	0,071128373
3,155	66,93	0	0
3,205	67,83	0	0
3,255	68,72	0,000021832	0,006445762
3,305	69,62	0	0
3,355	70,66	0	0
3,405	71,73	0,000363007	0,083508772
3,455	72,80	0,000486578	0,09574132
3,505	73,86	0,000372829	0,062621483
3,555	74,92	0,002578314	0,371104847
3,655	77,04	0,002367994	0,427437799
3,705	78,10	0,001780007	0,309604998
3,755	79,16	0,000184178	0,034955237
3,805	80,22	0,000161376	0,026743292
3,855	81,28	0	0
3,905	82,34	0	0
3,955	83,40	0	0
4,005	84,46	0	0
4,055	85,51	0	0
4,105	86,57	0,000144696	0,021491951
4,155	87,63	0,000160487	0,028911207
4,205	88,68	0,000184541	0,032017796
4,255	89,74	0,000067444	0,013079598
4,305	90,81	0,000236998	0,050782722
4,355	91,87	0,00021965	0,037227424
4,405	92,94	0,000427703	0,079890874
4,455	94,00	0,000751846	0,121368319
4,505	95,07	0,00060021	0,099695037
4,555	96,12	0,000287642	0,044471873
4,605	97,19	0,000583107	0,088193774
4,655	98,26	0,000327936	0,040901623
4,705	99,31	0,000117407	0,01836042
4,755	100,37	0	0
4,805	101,43	0,00013995	0,021254606
4,855	102,51	0	0
4,905	103,58	0,000185293	0,027648195
4,955	104,66	0,000161831	0,023465532
5,005	105,71	0	0
5,055	106,79	0,000128463	0,024757068
5,105	107,87	0	0
5,155	108,94	0	0
5,205	110,02	0	0
5,255	111,09	0,000843679	0,130675575
5,305	112,18	0,001430725	0,264793
5,355	113,28	0,000115917	0,023564158
5,405	114,39	0,000238705	0,045066709
5,455	115,50	0	0
5,505	116,61	0	0
5,555	117,73	0	0
5,605	118,85	0	0
5,655	119,99	0,000082835	0,013823732
5,705	121,13	0,000054369	0,009800223
5,805	123,41	0	0
5,855	124,57	0	0
5,905	125,86	0	0
5,955	127,33	0	0
6,005	128,75	0	0
6,055	129,91	0	0
6,105	130,88	0	0
6,205	132,68	0,000318324	0,060395763
6,255	133,54	0	0
6,295	134,21	0	0
6,345	135,03	0,000288125	0,063045159
6,395	135,88	0,000731103	0,144196557
6,445	136,71	0	0
6,505	137,72	0	0
6,545	138,39	0	0
6,605	139,41	0	0
6,655	140,26	0	0
6,705	141,11	0	0
6,755	141,98	0	0
6,805	142,87	0	0
6,855	143,75	0,000857475	0,110476255
6,905	144,62	0,000299595	0,05068363
6,955	145,51	0	0
7,055	147,29	0,001327375	0,20583235
7,105	148,18	0,000760231	0,097549841
7,155	149,09	0,000409292	0,061231326
7,205	149,98	0	0
7,255	150,89	0,000092371	0,022190843
7,305	151,79	0,000450116	0,054463923
7,355	152,70	0,002452377	0,304583564
7,405	153,60	0,001453503	0,163764488
7,455	154,49	0,002373634	0,373850536
7,555	156,31	0,001898102	0,243612149
7,605	157,21	0,001130433	0,142007325
7,655	158,12	0,00065809	0,103879588
7,705	159,02	0	0
7,755	159,93	0,000389162	0,062005338
7,805	160,83	0,001127847	0,106780043
7,855	161,73	0,000118888	0,020787385
7,905	162,62	0,000370543	0,060206726
7,955	163,50	0,002201686	0,301740588
8,005	164,39	0,000278085	0,052819412
8,055	165,26	0	0
8,105	166,14	0	0
8,155	167,03	0,000113431	0,021211327
8,205	167,91	0	0
8,255	168,79	0,000140631	0,021262694
8,305	169,65	0,000268573	0,031080504
8,355	170,51	0,00027742	0,031481512
8,405	171,38	0,000318511	0,05748188
8,455	172,22	0,001165646	0,201553528
8,505	173,06	0,002989926	0,369745717
8,555	173,39	0,001733979	0,2218206
8,605	173,39	0,001367189	0,154717739